NOTES AND CORRESPONDENCE

Zonal Jets Entering the Coral Sea

LIONEL GOURDEAU

Institut de Recherche pour le Développement, Nouméa, New Caledonia

WILLIAM S. KESSLER

NOAA/Pacific Marine Environmental Laboratory, Seattle, Washington

RUSS E. DAVIS AND JEFF SHERMAN

Scripps Institution of Oceanography, La Jolla, California

CHRISTOPHE MAES

Institut de Recherche pour le Développement, Nouméa, New Caledonia

ELODIE KESTENARE

LEGOS, Toulouse, France

(Manuscript received 21 February 2007, in final form 12 July 2007)

ABSTRACT

The South Equatorial Current (SEC) entering the Coral Sea through the gap between New Caledonia and the Solomon Islands was observed by an autonomous underwater vehicle (Spray glider) and an overlapping oceanographic cruise during July–October 2005. The measurements of temperature, salinity, and absolute velocity included high-horizontal-resolution profiles to 600-m depth by the glider, and sparser, 2000-m-deep profiles from the cruise. These observations confirm the splitting of the SEC into a North Vanuatu Jet (NVJ) and North Caledonian Jet (NCJ), with transport above 600 m of about 20 and 12 Sv, respectively. While the 300-km-wide NVJ is associated with the slope of the main thermocline and is thus found primarily above 300 m, the NCJ is a narrow jet about 100 km wide just at the edge of the New Caledonian reef. It extends to at least a 1500-m depth with very little shear above 600 m and has speeds of more than 20 cm s^{-1} to at least 1000 m. An Argo float launched east of New Caledonia with a parking depth fixed at 1000 m became embedded in the NCJ and crossed the glider/cruise section at high speed about 3 months before the glider, suggesting that the jet is the continuation of a western boundary current along the east side of the island and extends across the Coral Sea to the coast of Australia. In the lee of New Caledonia, the glider passed through a region of eddies whose characteristics are poorly understood.

1. Introduction

The South Equatorial Current (SEC) is the westward limb of the South Pacific subtropical gyre. It enters the Coral Sea primarily through the gap between New Caledonia and the Solomon Islands, and flows westward to the coast of Australia (Fig. 1). It bifurcates at the coast, one part flowing southward to become the East Australian Current, the other part flowing northward via the North Queensland Current into the Solomon Sea (Qu and Lindstrom 2002; Kessler and Gourdeau 2007). This latter pathway represents a principal water mass connection between the subtropical southwest Pacific and the equatorial ocean (Tsuchiya 1981); the possibility that transport changes along this pathway influence climate on the equator motivates study of the regional circulation.

Several sources of information have demonstrated

Corresponding author address: Lionel Gourdeau, IRD, BPA5 Nouméa, New Caledonia.
E-mail: lionel.gourdeau@noumea.ird.nc

DOI: 10.1175/2007JPO3780.1

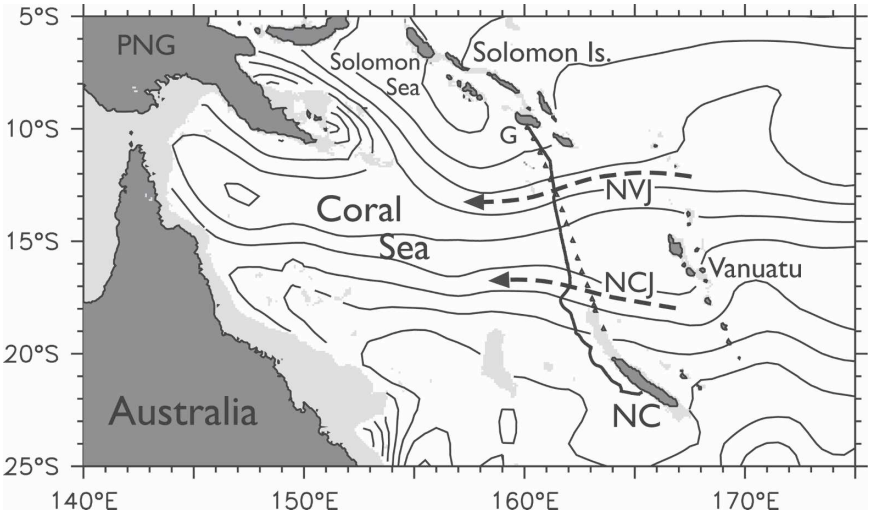

FIG. 1. Overview map of regional features of the southwest Pacific showing the track lines of the glider and cruise. Dark gray shading indicates land and light gray indicates ocean bottom less than 200 m deep. Islands referred to in the text are named NC (New Caledonia), G (Guadalcanal), and PNG (Papua New Guinea). The main tracks of the NVJ and NCJ are shown by dashed arrows, overlaid on contours of geostrophic streamlines at sigma-theta 25.5 from the CARS climatology. The glider track is shown by a heavy line from Guadalcanal to the west side of New Caledonia. The cruise track is shown by a dot where each CTD profile was made.

that the broad westward flow feeding the Coral Sea is broken into several jets (Fig. 1). Historical climatologies show zonal geostrophic jets extending west of the northern and southern tips of the large island groups of Fiji, Vanuatu, and New Caledonia (Qu and Lindstrom 2002; Ridgway and Dunn 2003; Kessler and Gourdeau 2007). These structures are also regularly depicted in OGCMs with sufficient horizontal resolution (Webb 2000). Stanton et al. (2001) confirmed with CTD and ADCP observations the presence of a very narrow jet south of Fiji. Although these jets mostly reflect the blocking effect of the islands on the SEC through "island rule" dynamics (Godfrey 1989), some of the filamentary structure is inherent in the wind forcing and occurs well east of the islands (Kessler and Gourdeau 2006).

Based on an OGCM and on the recent Commonwealth Scientific and Industrial Research Organisation (CSIRO) Atlas of Regional Seas climatology (CARS; Ridgway et al. 2002), Kessler and Gourdeau (2007) described the permanent jets passing north of Vanuatu and New Caledonia: the North Vanuatu Jet (NVJ) and the North Caledonian Jet (NCJ), centered at 13°S and 18°S, respectively (Fig. 1). In the climatologies, the jets have a maximum mean speed of about 10 cm s^{-1} and subsurface maxima with the core of the NVJ at 100-m depth and the core of the NCJ at 250-m depth, consistent with the north–south tilting of the subtropical gyre (Ridgway and Dunn 2003; Kessler and Gourdeau 2007).

There are few direct observations of the jets. Sokolov and Rintoul (2000) analyzed the only existing full-depth section across the Coral and Tasman Seas: the World Ocean Circulation Experiment (WOCE) P11S line from the tip of New Guinea, south along 154°–156°E in the western Coral Sea, sampled in June–July 1993. Taking geostrophic velocity relative to the bottom, they found peak speeds in the jet cores higher than climatology by a factor of 2 or more and zonal speeds greater than 10 cm s^{-1} extending to about 800-m depth.

The purpose of this study is to document the inflow entering the Coral Sea through the gap between New Caledonia and the Solomon Islands based on several types of nearly synoptic direct observations during a coordinated sampling effort in July–October 2005. An oceanographic cruise called Secalis3 provided temperature and salinity profiles and lowered acoustic Doppler current profiler (L-ADCP) velocity measurements to 2000 m at intervals of about 70 km, while an underwater glider running nearly the same track measured temperature and salinity to 600 m on a fine spatial scale as well as produced a section of vertically averaged velocity based on its measured motion. Complementary information is given by one autonomous float of the Argo array that was advected through the NCJ a few months earlier. Results from these direct observations are dis-

cussed with regard to the climatology and to island rule dynamics. Since the Solomon Islands north of Guadalcanal are connected by a reef system with only very shallow and narrow passages, the transport sampled here represents virtually all the flow entering the Coral Sea over the latitude range 23°–5°S (Fig. 1).

2. Data

a. Spray glider

The Spray glider is a 2-m, 52-kg autonomous underwater glider that cycles vertically through the water column by changing its volume like an Argo float (Roemmich et al. 2004) and uses lift on its wings to convert part of this vertical velocity into forward motion. The glider's position is determined by GPS at each surfacing, and each dive's data are reported immediately through Iridium satellites. Two complementary types of data are produced by the glider: profiles of temperature and salinity comparable to Argo float data, and an estimate of absolute depth-averaged velocity derived from the difference between vehicle motion as measured by GPS fixes and the distance traveled through the water. The glider measures pressure and heading every 8 s, computes its vertical velocity from pressure, and uses a field- and laboratory-verified model of gliding dynamics to infer horizontal velocity through the water, which is integrated over the dive. To the extent that vertical ocean velocities average to zero and drift at the surface does not contaminate the measurement of distance traveled through the water (see next section), a uniform glider vertical velocity leads to equal sampling at all depths. With vehicle velocity through the water known, the difference between dead-reckoning displacement and distance traveled gives the absolute vector ocean velocity averaged over the glider's operating depth range (Fig. 2). The Spray glider was developed at Scripps in collaboration with Woods Hole scientists (Sherman et al. 2001) and is described by Davis et al. (2002) and Rudnick et al. (2004).

Spray glider 1 was deployed on 17 July 2005 during the Secalis3 oceanographic cruise just offshore of Guadalcanal Island (9°55.39′S, 160°9.58′E) in the southern Solomon Islands to follow nearly the same path as the Secalis3 section (Fig. 2). Spray cruises at 20–25 cm s^{-1} along a saw-toothed path with typical glide angles of 17° from the horizontal, so that each of the 600-m dives on this mission took about 4 h and covered 3 km horizontally. It was recovered 3 months later on 17 October 2005 just outside the New Caledonian reef (21°42.21′S, 165°22.24′E) by a small team in a dinghy, after covering a total distance of 1640 km (Fig. 2). The 3-month track yielded a section of 573 temperature–salinity (T–S) profiles, and estimates of 0–600-m depth-averaged velocity that were highly resolved in space but also nonsynoptic in time.

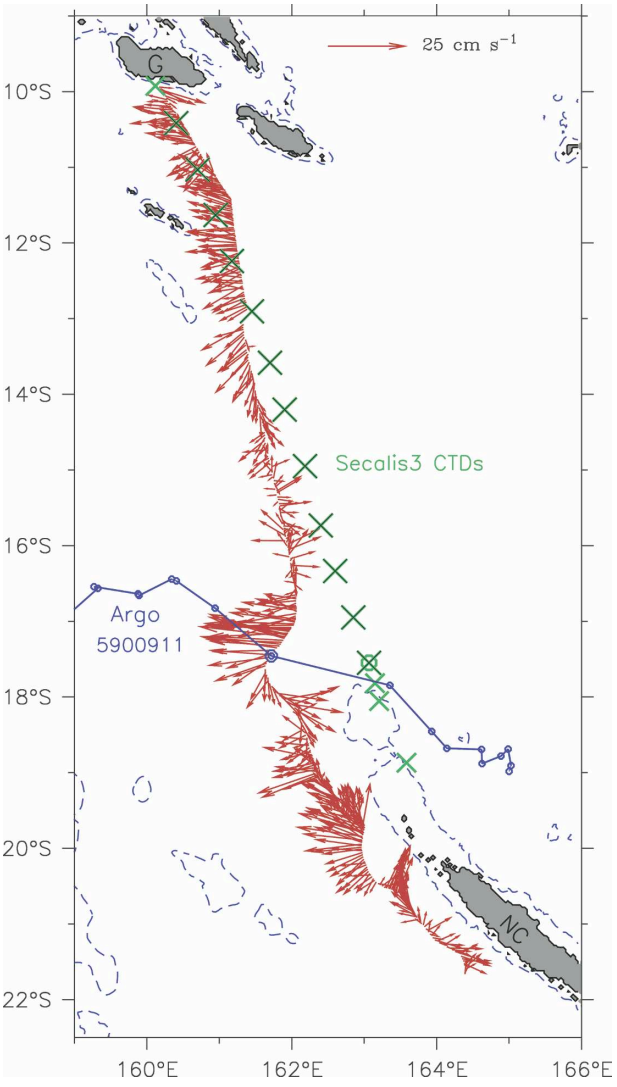

FIG. 2. Observations made during this study: absolute velocity (red vectors) averaged over the upper 600 m, measured by the glider for each dive, is shown along the glider section between Guadalcanal and New Caledonia (marked with G and NC). Superimposed are the locations of the 17 Secalis3 stations extending to 2000-m depth (crosses; the one at 17.55°S overlaid with a circle indicates the L-ADCP profile shown in Fig. 6). The trajectory and profile locations of the Argo float 5900911 are in blue. Land is shaded gray and the 500-m isobath is the blue dashed contour, showing the northward extension of the reef at the extremity of New Caledonia.

1) ERROR SOURCES IN THE GLIDER MEASUREMENTS

A factory calibrated Sea Bird 41-CP CTD, specifically configured for use on gliders using a pumped-

water system, was installed in Spray 1. Unfortunately, an error in the installation instructions led to the conductivity cell's central electrode (rather than the outer electrodes as intended) being held at the vehicle's ground potential. This allowed an unintended electrical path that affected calibration. In a spot precruise check (expected accuracy ~0.05 psu) the installed CTD read too fresh by 0.08 psu. Comparison of Spray profiles with the Secalis3 data, CARS climatology, and a single Argo float showed agreement among temperature measurements but a consistent 0.09-psu fresh bias in the reported Spray salinities. Whether this is an effect of the wiring polarity inversion (yet the sense seems wrong) or some postcalibration occurrence remains unclear, but all results reported here have been corrected by adding 0.09 to salinity. Although this introduces doubt into the salinity section itself, the constant offset has a negligible effect on the geostrophic velocities computed using these values.

Errors on the estimation of the glider-measured currents depend on several factors. Except in frontal regions, oceanic vertical velocities averaged over the depth and duration of a dive are $O(1\ \mathrm{mm\ s^{-1}})$ and contribute a negligible error to measured currents, mainly to the along-track component. Spray's vertical velocity decreases during descent by 10%–15% but is controlled to near a constant value on ascent. Consequently, the "depth-average" velocity weights deep depths 5%–7% more than shallow depths and is presumably biased low, compared with uniform weighting, by a comparable amount.

After reaching the surface, Spray increases buoyancy for better GPS/Iridium communication, gets a GPS fix, communicates through Iridium, gets a second GPS fix, and reduces its volume to descend. Motion between the two GPS fixes is measured but the surface drift before and after the fixes can only be estimated. The total time spent at the surface is about 15 min while the time between fixes is one-third of this. Depth-average velocity was computed two ways: (i) excluding only the measured surface motion and (ii) using surface drift velocity from the GPS fixes to exclude the measured surface drift plus that from 10 min of drifting not measured by the GPS fixes. The difference between the two estimates of mean cross-track and along-track depth-average velocity over the 1640-km track is $O(2\ \mathrm{mm\ s^{-1}})$ (3%–4% of the mean depth-averaged velocity).

The most serious inaccuracy in measured transport comes from the vehicle's flux gate compass, which has typical errors of 3° (peak of 5°) that vary with heading on a correlation scale of 45° to 180° and change when new batteries are installed. Spray 1 had not been fitted with a heading-dependent compass correction table, so the compass contributes typical errors of 5% of the vehicle velocity to the measured cross-track currents. Even with significant reduction of these errors by averaging as the vehicle changes heading, the mean-velocity error from the compass is likely $O(5)\ \mathrm{mm\ s^{-1}}$.

These different errors on the estimation of the glider-measured currents could produce up to a 6-Sv (1 Sv $\equiv 10^6\ \mathrm{m^3\ s^{-1}}$) error on the cross-track transport above 600 m between Guadalcanal and New Caledonia.

2) DATA FILTERING

The high-density sampling of the glider resolved a short-scale oscillation in most of the fields; this amounted to about 2 dyn-cm rms in the dynamic height, superimposed on the large-scale signature of more than 20 dyn-cm. However, since the transport depends on the end-to-end dynamic height difference, the small-scale oscillations could produce an uncertainty up to 1–2 Sv for the cross-track transport above 600 m between Guadalcanal and New Caledonia. The time-lagged structure function shows that dynamic height is dominated by 12-h variability with a bandwidth of about ¼ $\mathrm{day^{-1}}$. We hypothesize that this variability is a consequence of a combination of solar and lunar semidiurnal internal tides that modulate the density field. A combination of the movement of Spray through the finite-wavelength internal waves and variability of currents between the internal wave's source and the observation point could broaden the bandwidth of this signal. Under the assumption that the high-frequency variability of dynamic height results from the semidiurnal tide, a filter was constructed to remove this tidal signal. Taking the dataset of dynamic heights to be the vector $\mathbf{d}$, the filter output is $\hat{\mathbf{d}} = A\mathbf{d}$, where the filter weights A are chosen to completely remove any signal of the form $\sin(\omega t + \phi)$, where ω is two cycles per day, and ϕ is the phase angle. This was done by minimizing (in the manner of objective mapping) the mean square error $\langle |\mathbf{d} - \hat{\mathbf{d}}|^2 \rangle$ when the time-lagged covariance of dynamic height is stationary (in time) and has the form $\exp(-t^2/2\tau^2)$, where τ was chosen to be 1.5 days. Subsequent geostrophic velocity and transport from the glider are based on the filtered data.

b. Cruise data

Oceanographic cruises are being carried out by the Institut de Recherche pour le Développement (IRD) center at Nouméa with the objective of documenting the mass fluxes and circulation between the archipelagos of the southwest Pacific, as part of the International South Pacific Circulation Experiment (SPICE; see online at http://www.ird.nc/UR65/SPICE/). The Secalis3

cruise was conducted during 11–24 July 2005 between New Caledonia, Santo (Vanuatu), and Guadalcanal (Solomon Islands), on board the R/V *Alis*. Between the northern extremity of New Caledonia and Guadalcanal Island, the section of interest for this study, 17 shipboard profiles of temperature, salinity, and oxygen were obtained with a Sea Bird SBE 911+ CTD probe from the surface to 2000-m depth at intervals of about 70 km (Fig. 2). Current profiles (0–2000 m) were also obtained from two RD Instruments 300-kHz L-ADCPs attached to the rosette, one looking downward and the other looking upward. The R/V *Alis* is also equipped with a vessel-mounted (VM)-ADCP (broadband, 150 kHz), which provides velocity profiles in the first 250-m depth continuously. Temperature and conductivity from Secalis3 CTD sensors have been pre- and post-calibrated, and a linear fit is applied to the salinity dataset using the calibration values. The accuracy of the salinity data is estimated at ± 0.0025 by comparison with salinity analysis from water samplings at 2000 m. Direct comparison with the Argo float that crossed the cruise track (see section 2c below) is possible at 17°S, where both Argo and Secalis3 temperature–salinity relationships compare very well after cross-validating these data obtained in the same month (July 2005). Secalis3 temperature and salinity data have also been checked against the CARS climatology at depth, where Secalis3 data and the averaged July–September CARS climatology are similar. Only the first few L-ADCP profiles are available because of the failure of the pressure case during the cruise. Fortunately this included a profile near the center of the narrow NCJ (the green circle in Fig. 2). L-ADCP measurements were processed following the method described by Visbeck (2002), and the final profiles are also constrained in the surface layers by the VM-ADCP measurements. Detailed information about the cruise, CTD calibration, and L-ADCP processing is given in the cruise report (Gourdeau et al. 2007).

c. Argo float data

An additional source of information is provided by the presence of one Argo float [World Meteorological Organization (WMO) ID 5900911] deployed on 23 April 2005 at 19°S, 165°E during the IRD cruise Frontalis3. With a parking depth fixed at 1000 m, the trajectory of this float, given by its location every 10 days when it rises to the surface, shows that it was caught up in the NCJ and advected into the Coral Sea (Fig. 2). Coincidentally, the Argo float surfaced and made a profile right on the glider track at 17.46°S, 161.7°E on 14 July 2005, 48 days before the glider sampled the same location.

d. CARS

The CSIRO Atlas of Regional Seas compilation was produced by Ridgway et al. (2002) from more than 65 000 temperature and salinity profiles in the region 10°N–50°S, 100°E–180° using a locally weighted least squares mapping. The compilation uses a topographic weighting to minimize contamination of deeper oceanic regions by continental shelf waters, with an additional weighting function to avoid interpolation across topographic barriers. CARS fields are produced on a ½° latitude–longitude grid with 56 vertical levels.

e. Island rule

The Godfrey (1989) island rule is a generalized Sverdrup streamfunction that determines the total meridional transport between an island and the coast to its east (thus including the western boundary transport along the island's coast), using the interior wind-driven Sverdrup flow plus the assumption of cross-stream geostrophy in western boundary currents (see also Wajsowicz 1993 and Pedlosky et al. 1997). Working west from South America, and then from island to island (including Australia), a complete generalized Sverdrup streamfunction field can be estimated from the surface wind only. Wind data from the European Remote Sensing Satellite (ERS) scatterometer are used to infer this island rule transport. The winds used here were processed into monthly 1° latitude × 1° longitude gridded fields of stress components by the Centre ERS d'Archivage et de Traitement (CERSAT) and obtained from their Web site (see http://www.ifremer.fr/cersat). A monthly average annual cycle was constructed from the 9.5 yr of data (1991–99), and the mean of that cycle was used for the curl and island rule transport. Quick Scatterometer (QuikSCAT) winds (Schlax et al. 2001) for the period 2000–05 have also been used to test the sensitivity of the island rule calculation. The QuikSCAT winds have also been used to estimate the Ekman transport during July–September 2005.

3. Results

For the remainder of this paper, we will be concerned with SEC flow through the gap between the northern tip of the New Caledonia reef at 18°S and Guadalcanal at 10°S (Figs. 1, 2). As noted above, this encompasses virtually all the transport entering the Coral Sea over the much larger range 23°–5°S. The glider provides an estimate of the 0–600-m vertically averaged velocity, and the cross-track geostrophic velocity relative to 600 m. The difference between the vertical average of cross-track geostrophic velocity and of glider-measured absolute velocity gives the reference level cross-track

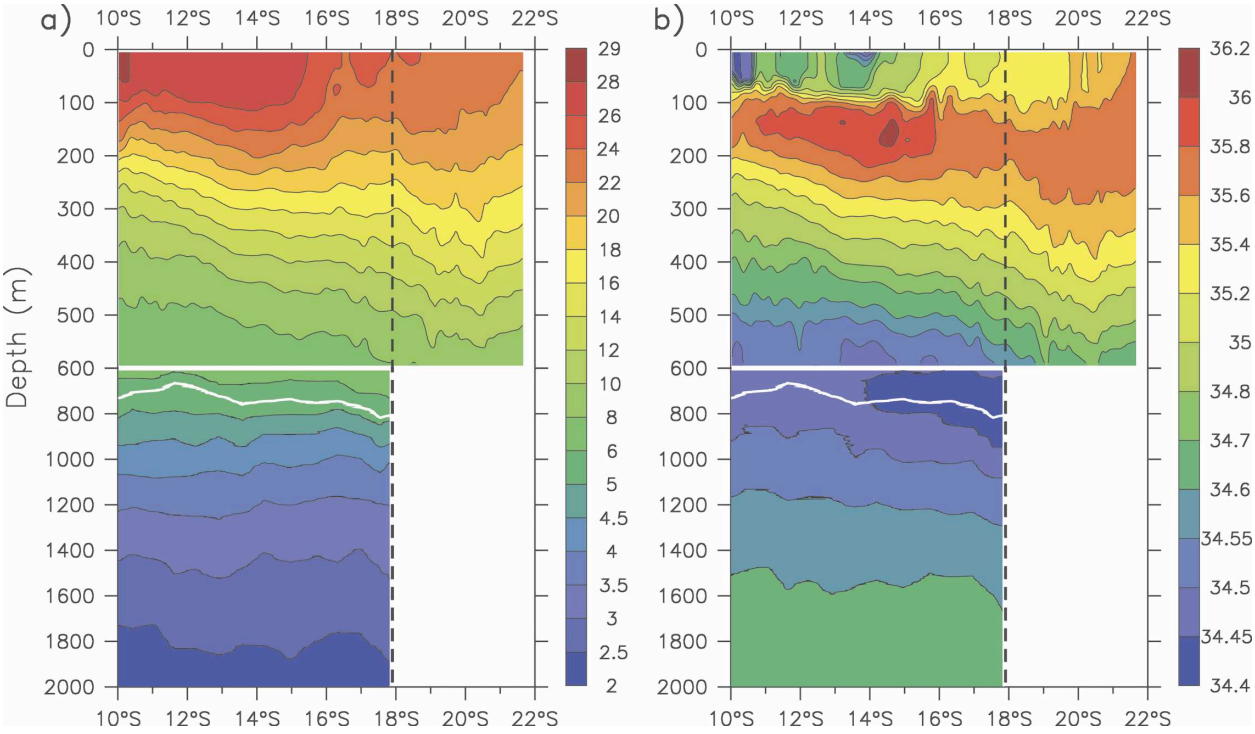

FIG. 3. Sections of (a) temperature and (b) salinity along the track from Guadalcanal in the north (left side of plots) to New Caledonia in the south. Note stretched vertical scale. The upper 600-m values are from the glider, and extend down the west side of New Caledonia (the vertical dashed line indicates the reef edge at 18°; see Fig. 2). Values below 600 m are from the cruise CTDs and stop at the northern tip of the reef. The white line near 700-m depth is the sigma-theta 27.2 contour.

velocity and thus the absolute geostrophic cross-track velocity over the upper 600 m. The Secalis3 cruise provides geostrophic cross-track velocity relative to 2000 m. Since the tracks are almost meridional (its direction is about 10° from due north), this is nearly the zonal component. Transport values cited hereafter are positive eastward across the track.

Vectors of absolute vertically averaged velocity for each dive along the glider section (Fig. 2) show two westward jets: a broad NVJ extending from about 10°–14°S, and a thin NCJ that rounds the extensive reef system extending north of New Caledonia at 17°–18°S. These two jets are the dominant features of the SEC when it enters the Coral Sea. Note that the westward digression of the glider when crossing the NCJ reveals its inability to maintain its course across such a strong current. A narrow eastward current is embedded along the southern Guadalcanal coast. Between the two jets, in the lee of Vanuatu (about 400 km east of the track; Fig. 1), there is a band of less-organized, generally eastward flow. In the immediate lee of New Caledonia, the glider passed through a region of mesoscale currents suggestive of a series of strong eddies whose origin and properties are unknown, and that may be partly associated with gaps in the northern reef (Fig. 2).

The surface signature of dynamic height relative to 600 m shows a 20 dyn-cm amplitude for the NVJ, quite in accord with the climatology. Such a signature is not so obvious for the NCJ because it has only a 5 dyn-cm signature visible in the 600-m glider hydrography. This reflects the characteristics of the upper thermocline (isotherms from about 14°–24°C), which slopes down to the south until 14°S, then slopes increasingly upward to the New Caledonia reef edge at 18°S (Fig. 3a). The geostrophic shear due to the thermocline slope produces the relatively shallow NVJ, which is clearly seen in 0–600-m geostrophy, but the shallow geostrophic shear is generally eastward south of 14°S, with only a weak and narrow signature of the NCJ at 17°S (Fig. 4, top panel). The geostrophic cross-track transport is very sensitive to the selection of the reference level of no motion. Relative to a 600-m level of no motion, the geostrophic 0–600-m cross-track transport from either the glider or the shipboard temperature and salinity profiles is only about half of the total value directly estimated between the Solomon Islands and New Caledonia by the glider track, with most of the difference in the NCJ region between 16° and 18°S (Fig. 5).

Isotherms deeper than 14°C and also isohalines at these levels continue to slope down to the south (but

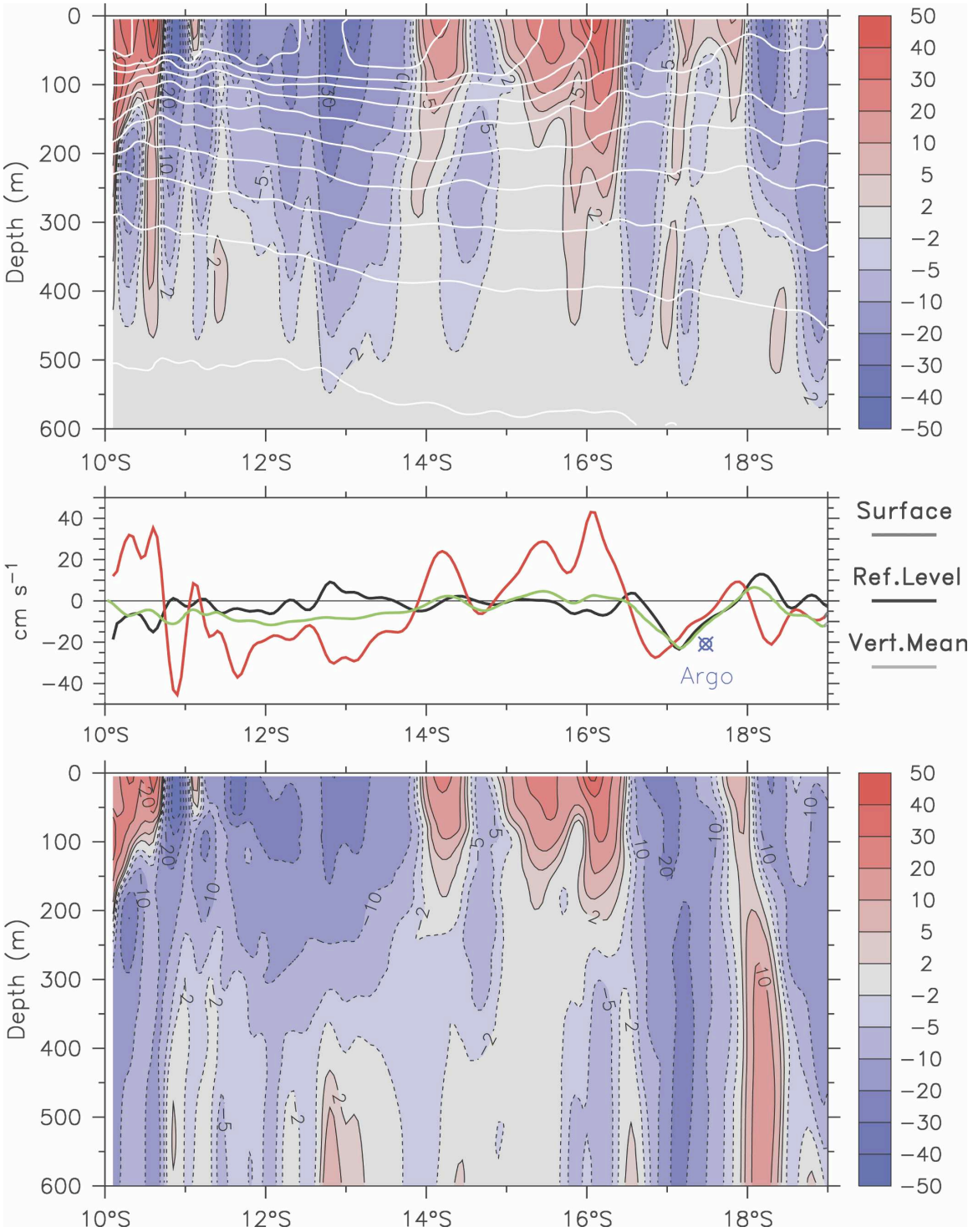

FIG. 4. Cross-track geostrophic velocity (u_g; cm s^{-1}) determined by the glider. (top) The u_g relative to 600 m (red indicates eastward and blue westward), with overlaid white contours of sigma-theta. (middle) Absolute cross-track u_g (see text) at the reference level (black line), at the surface (red), and at the vertical average (green). The blue dot is the drift speed of Argo float 5900911 when it crossed the glider track (see Fig. 2). (bottom) Absolute cross-track u_g.

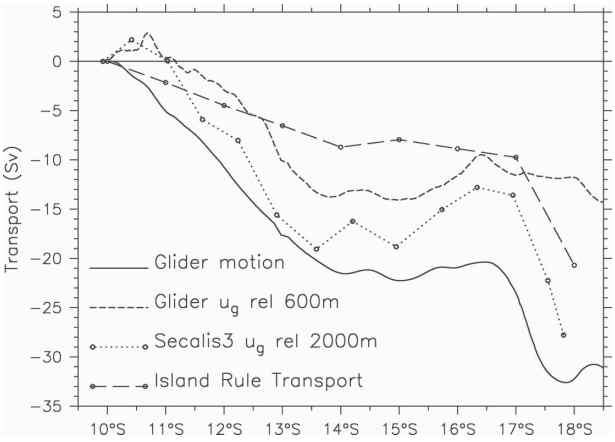

FIG. 5. Cumulative cross-track transport (Sv) integrated southward along the section from the glider's measured motion (solid), glider geostrophy relative to 600 m (dashed), Secalis3 cruise geostrophy relative to 2000 m (dotted; values at large dots), and island rule transport (long dashes).

note that between the high-salinity core at about 175 m and the salinity minimum near 700 m, the gradients of temperature and salinity tend to cancel; Fig. 3). Right at the New Caledonia reef edge, the downward slope to the south of both isotherms and isohalines below the salinity minimum produces a narrow band of westward geostrophic shear extending to the deepest observations of Secalis3 at 2000 m. The significance of the slopes is quantified by noting that if Secalis3 dynamic height is computed relative to 1126 m, only half the NCJ transport results. When absolute vertically averaged velocity derived from the glider motion is used to reference the geostrophic shear (black curve in Fig. 4, middle panel), relatively little modification is made to the NVJ (and that primarily is at the far northern end of the section), but the NCJ appears as a deep, narrow, westward-moving column that is virtually barotropic over the upper 600 m (Fig. 4, bottom panel). The strong flow of the NCJ is therefore understood as essentially due to these very deep structures, and not to the shape of the main thermocline. Although the bottom depth below the NCJ is about 4500 m, the fact that the geostrophic transport relative to 2000 m from the Secalis3 CTD profiles is close to the absolute transport from the glider (Fig. 5) suggests that flow below 2000 m is relatively weak.

The integral of absolute cross-track glider velocity over 0–600 m from Guadalcanal to the New Caledonian reef gives a total of −32 Sv entering the Coral Sea (Fig. 5). A counterflow just south of the reef edge (Figs. 2, 4) produces a roughly 2-Sv ambiguity in the glider-measured Guadalcanal–New Caledonia transport total. About −20 Sv are transported in the 300-km-wide NVJ, and the rest in the 100-km-wide NCJ. The −32-Sv total (0–600 m) is about 10% larger than the Secalis3 0–2000-m cross-track transport relative to a 2000-m level of no motion, which also shows a band of eastward flow at 15°–16°S that is barely evident in the glider velocity (Fig. 4). Possible explanations for the difference include accumulation of glider compass errors or the reliance of the shipboard estimate on the single profile right at the reef edge, which might have been aliased by tides or other high-frequency signals. The glider and ship tracks also diverge by about 150 km at their southern ends where the current is most intense (Fig. 2). The difference might also be accounted for by the Ekman transport, which is included in the glider motion estimate but excluded from the shipboard geostrophy. Cross-track Ekman transport during July–September 2005 is estimated at −2.5 Sv based on contemporaneous QuikSCAT winds; because the winds are easterly and nearly perpendicular to the track, the cross-track Ekman transport is relatively small.

Two comparable estimates of transport through the Guadalcanal–New Caledonia gap are available from climatological data. The first-order wind-driven description of the steady circulation is the Godfrey (1989) island rule (see section 2d), which gives a transport of about −21 Sv across this section, with the discrepancy coming primarily from a much weaker NVJ (Fig. 5). CARS geostrophic transport, relative to a 2000-m level of no motion, totals about −24 Sv. The roughly 25% larger values found from the present observations compared with either of these historical sources is probably larger than the seasonal cycle could account for (Kessler and Gourdeau 2007), though this is likely to be a factor since the sampling occurred near the seasonal transport maximum. While the island rule is a steady balance and cannot strictly be used to study time evolution, a test calculation using QuikSCAT winds for the period 2000–05 shows an about −4 Sv increase over the results estimated with the ERS 1991–99 mean as shown in Fig. 5, with most of the increase in the NVJ, suggesting that interannual variations may contribute as well. CARS geostrophic transport relative to a 2000-m level of no motion also shows the double-jet structure, though its NCJ is spread out over 4° latitude and does not extend as deep.

The observed feature of the NCJ extending in the deep ocean is supported by other datasets. The L-ADCP velocity profile at 17.55°S (Fig. 6) confirms the picture from geostrophy, with consistent westward speeds from about 20 cm s^{-1} down to 1100 m. Serendipitously, an Argo float deployed east of New Caledonia about 3 months before the glider mission, was taken up in the NCJ, and was advected past the glider

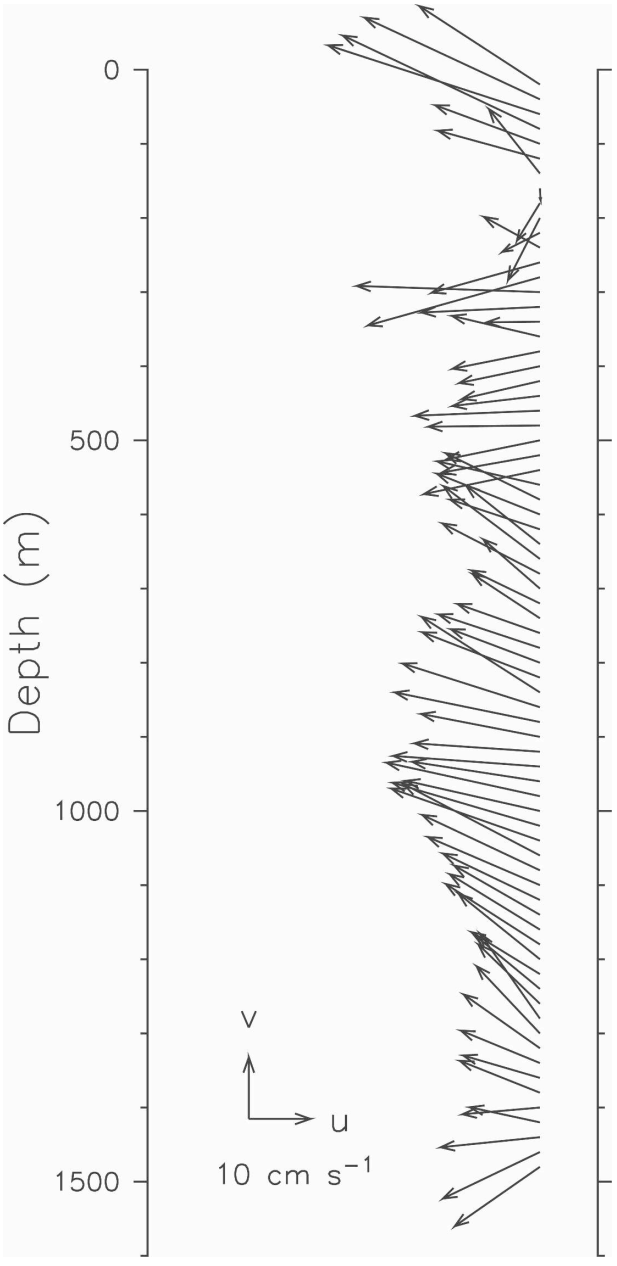

FIG. 6. Velocity measured by the L-ADCP in the center of the NCJ at 17.55°S. Eastward currents plotted to right, northward up (see scale key).

section (Fig. 2). Its velocity intensified as it passed the north extremity of the reef with a mean speed of −21 cm s^{-1} during its 10-day submergence at 1000-m depth, consistent with speeds measured by the glider and shipboard L-ADCP (Fig. 4, dot in middle panel). (This was about twice as fast as the float speed just before and just after this interval, and about 5 times faster than its mean speed over a year.) After passing the New Caledonia reef, the Argo float has continued almost due west along 17°S (though interrupted by several eddies) and was approaching the coast of Australia as of 30 June 2006, with a net displacement of 1500 km in 433 days (−4 cm s^{-1}). This track and speed is consistent with westward geostrophic currents measured at 17°S just east of the Australian shelf on WOCE section P11 (Sokolov and Rintoul 2000). Such a velocity estimate is also consistent with the mean circulation deduced from the Autonomous Lagrangian Current Explorer (ALACE) float displacements at the intermediate depth, near 900 m (Davis, 2005). Thus, three independent, nearly synoptic data sources (glider, shipboard L-ADCP, and the Argo float) backed by previous data reveal a new description of a strong, deep NCJ as a quasi-barotropic jet, whose flow extends far westward into the Coral Sea. It is noted that XBT measurements along the commercial ship lines crossing the Coral Sea from New Caledonia to the Solomon Sea cannot depict the NCJ because measurements are not deep enough (500 m).

Just south of the NCJ jet (past the tip of the reef), the glider crossed a narrow eastward flow with vertically averaged speeds up to 14 cm s^{-1} (Fig. 2), nearly as large as that of the jet itself, though its transport was much smaller (Fig. 5). Then at 19°S it crossed another flow of similar magnitude, but to the west (Fig. 2). This coincides with the position of a 400-m-deep gap in the reef ("Le Grand Passage"), and there appears to be some westward flow through this strait. Transport from glider motion is about −3 Sv, and an L-ADCP profile made just on the east side of the gap (not shown) indicates westward flow of more than −20 cm s^{-1} at 200–300-m depth. On the other hand, this complex velocity structure may represent an eddy field generated as the jet separates from the reef, which confuses our picture of the NCJ itself.

4. Conclusions

The southwest Pacific between New Caledonia and the Solomon Islands has been sampled both during an oceanographic cruise and by an autonomous underwater glider, providing unique near-synoptic pictures of the SEC inflow entering into the Coral Sea. The glider produced highly resolved sampling of temperature and salinity in the upper 600 m, and a measure of the absolute vertically averaged velocity. The Secalis3 cruise provided hydrographic data from the surface down to 2000 m, with a few L-ADCP profiles in crucial regions. Its cross-track geostrophic velocity (relative to 2000 m) compares well with the absolute geostrophic velocity from the glider; the combination gives a detailed snapshot of the circulation for the July–October 2005 pe-

riod. The primary finding is that flow structures of the SEC in this region extend to great depth; in particular, a jet rounding the northern reef of New Caledonia has appreciable magnitude as deep as 1000 m.

These data also demonstrate that the SEC is split into two branches: the North Vanuatu Jet and the North Caledonia Jet, as predicted by the island rule (Godfrey 1989). Total westward transport through the gap between the Solomon Islands and New Caledonia is −32 Sv, comparable to that estimated previously along the P11S WOCE section occupied in 1993, 800 km to the west (Sokolov and Rintoul 2000), but larger by 25% than indicated by historical hydrographic data compilations and a Sverdrup model driven by winds during the 1990s. Taking into account the extensive shallow reef system surrounding these island groups, the measured −32 Sv is the total transport approaching the western boundary of the South Pacific between 23° and 5°S at this time. The NVJ is characterized by a high-salinity core at thermocline depth, originating from the southeast Pacific (Hanawa and Talley 2001), which could be a useful tracer of this water mass into the Coral and Solomon Seas.

This study provides a new description of the NCJ from those based on climatology and OGCM experiments (Kessler and Gourdeau 2007), which show a relatively broad flow. Here, the NCJ was directly observed as a very thin structure just at the edge of the northern New Caledonian reef, characterized by high velocity over a large vertical extent, with speeds from −20 cm s^{-1} to at least 1000 m, and little shear above this depth. The mass transport of this quasi-barotropic jet is about −12 Sv in the upper 600 m.

Along the eastern coast of New Caledonia, northward high velocities from the L-ADCP are observed. Thus, the NCJ appears as the westward continuation of a western boundary current along the east coast of New Caledonia. Along the west coast of New Caledonia, the complex velocity structure may represent an eddy field generated as the jet separates from the reef, which confuses our picture of the NCJ itself. West of the island, the flow continues across the Coral Sea, as established by the trajectory of an Argo float embedded in the jet, which traversed the breadth of the Coral Sea to approach the coast of Australia at an average speed of −4 cm s^{-1} over almost a year. The NCJ happens to be centered at the mean latitude of the bifurcation of the SEC at the Australian coast (18°S). Therefore, its large deep transport could have downstream implications in the redistribution of water masses at the western boundary.

The synergy shown in this study between relatively inexpensive observations with fine spatial scale from the underwater glider and more accurate and complete but spatially coarse ship-based measurements suggests how the combination can be used to observe both the structure and variability of large-scale current systems. A second similar mission is now in progress, with Spray 1 deployed during the recent Secalis4 oceanographic cruise (7–22 November 2006), and we plan regular monitoring of this section and others in the region.

Acknowledgments. We thank the captain and crew of the R/V *Alis* for skillfully deploying the glider and making the CTD/L-ADCP profiles during the Secalis3 cruise. Engineers Jean-Yves Panché and David Varillon of IRD Nouméa conducted the at sea operations. The Instrument Development Group at Scripps developed and prepared Spray and processed its data. Discussions with Meghan Cronin, Greg Johnson, and Dennis Moore of PMEL and Alex Ganachaud of IRD helped clarify some of the ideas presented here.

REFERENCES

Davis, R. E., 2005: Intermediate-depth circulation of the Indian and South Pacific Oceans measured by autonomous floats. *J. Phys. Oceanogr.,* **35,** 683–707.

——, C. E. Eriksen, and C. P. Jones, 2002: Autonomous buoyancy-driven underwater gliders. *The Technology and Applications of Autonomous Underwater Vehicles,* G. Griffiths, Ed., Taylor and Francis, 324 pp.

Godfrey, J. S., 1989: A Sverdrup model of the depth-integrated flow for the world ocean allowing for island circulations. *Geophys. Astrophys. Fluid Dyn.,* **45,** 89–112.

Gourdeau, L., A. Ganachaud, E. Kestenare, J. Y. Panché, and D. Varillon, 2007: Rapport de la mission Secalis 3 à bord du Navire Océanographique l'Alis: 11 juillet—24 juillet 2005, 22°S–9°55S, 160°07E–168°10E. Centre IRD de Nouméa, BP A5, New Caledonia, Rapports de Mission Sciences de la Mer 21, 80 pp.

Hanawa, K., and L. D. Talley, 2001: Mode waters. *Ocean Circulation and Climate*: *Observing and Modelling the Global Ocean,* G. Siedler, J. Church, and J. Gould, Eds., Academic Press, 373–386.

Kessler, W. S., and L. Gourdeau, 2006: Wind-driven zonal jets in the South Pacific Ocean. *Geophys. Res. Lett.,* **33,** L03608, doi:10.1029/2005GL025084.

——, and ——, 2007: The annual cycle of circulation of the southwest subtropical Pacific, analyzed in an ocean GCM. *J. Phys. Oceanogr.,* **37,** 1610–1627.

Pedlosky, J., L. J. Pratt, M. A. Spall, and K. R. Helfrich, 1997: Circulation around islands and ridges. *J. Mar. Res.,* **30,** 1199–1251.

Qu, T., and E. J. Lindstrom, 2002: A climatological interpretation of the circulation in the western South Pacific. *J. Phys. Oceanogr.,* **32,** 2492–2508.

Ridgway, K. R., and J. R. Dunn, 2003: Mesoscale structure of the mean East Australian Current system and its relationship with topography. *Prog. Oceanogr.,* **56,** 189–222.

——, ——, and J. L. Wilkin, 2002: Ocean interpolation by four-dimensional weighted least squares—Application to the wa-

ters around Australasia. *J. Atmos. Oceanic Technol.,* **19,** 1357–1375.

Roemmich, D., S. Riser, R. Davis, and Y. Desaubiez, 2004: Autonomous profiling floats: Workhorse for broad-scale ocean observations. *J. Mar. Technol. Soc.,* **38,** 2–21.

Rudnick, D. L., R. E. Davis, C. C. Eriksen, D. Fratantoni, and M. J. Perry, 2004: Undersea gliders for ocean research. *J. Mar. Technol. Soc.,* **38,** 73–84.

Schlax, M. G., D. B. Chelton, and M. H. Freilich, 2001: Sampling errors in wind fields constructed from single and tandem scatterometer datasets. *J. Atmos. Oceanic Technol.,* **18,** 1014–1036.

Sherman, J., R. E. Davis, W. B. Owens, and J. Valdes, 2001: The autonomous underwater glider 'Spray.' *IEEE J. Oceanic Eng.,* **26,** 437–446.

Sokolov, S., and S. Rintoul, 2000: Circulation and water masses of the southwest Pacific: WOCE section P11, Papua New Guinea to Tasmania. *J. Mar. Res.,* **58,** 223–268.

Stanton, B., D. Roemmich, and M. Kosro, 2001: A shallow zonal jet south of Fiji. *J. Phys. Oceanogr.,* **31,** 3127–3130.

Tsuchiya, M., 1981: The origin of the Pacific Equatorial 13°C water. *J. Phys. Oceanogr.,* **11,** 794–812.

Visbeck, M., 2002: Deep velocity profiling using lowered acoustic Doppler current profilers: Bottom track and inverse solutions. *J. Atmos. Oceanic Technol.,* **19,** 794–807.

Wajsowicz, R. C., 1993: The circulation of the depth-integrated flow around an island with application to the Indonesian Throughflow. *J. Phys. Oceanogr.,* **23,** 1470–1484.

Webb, D. J., 2000: Evidence for shallow zonal jets in the South Equatorial Current region of the southwest Pacific. *J. Phys. Oceanogr.,* **30,** 706–720.